RSC Advances

This article can be cited before page numbers have been issued, to do this please use: T. S. Khan, S. Gupta, M. I. Alam and M. A. Haider, *RSC Adv.*, 2016, DOI: 10.1039/C6RA22303F.

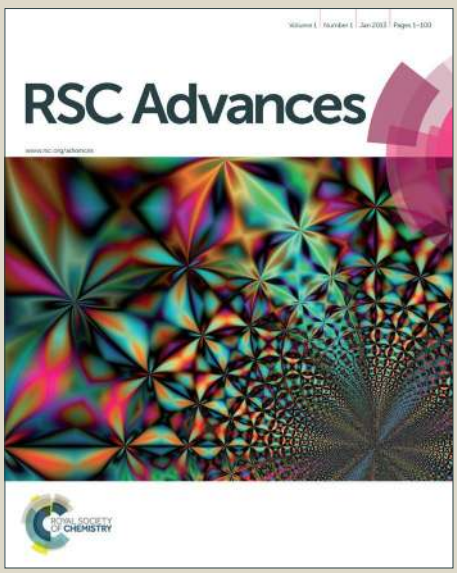

ROYAL SOCIETY OF CHEMISTRY

www.rsc.org/advances

View Article Online
DOI: 10.1039/C6RA22303F

Reactivity Descriptor for Retro Diels-Alder Reaction of Partially Saturated 2-Pyrones: DFT Study on Substituents and Solvents Effect

Tuhin S. Khan[1,*], Shelaka Gupta[1], Md. Imteyaz Alam[1] and M. Ali Haider[1,*]

[1] *Renewable Energy and Chemicals Laboratory, Department of Chemical Engineering, Indian Institute of Technology Delhi, Hauz Khas, New Delhi-110016*

**Corresponding Author*

Tel: +91-11-26591016, Fax: +91-11-2658-2037

E-mail: suvratuhin@gmail.com, haider@iitd.ac.in

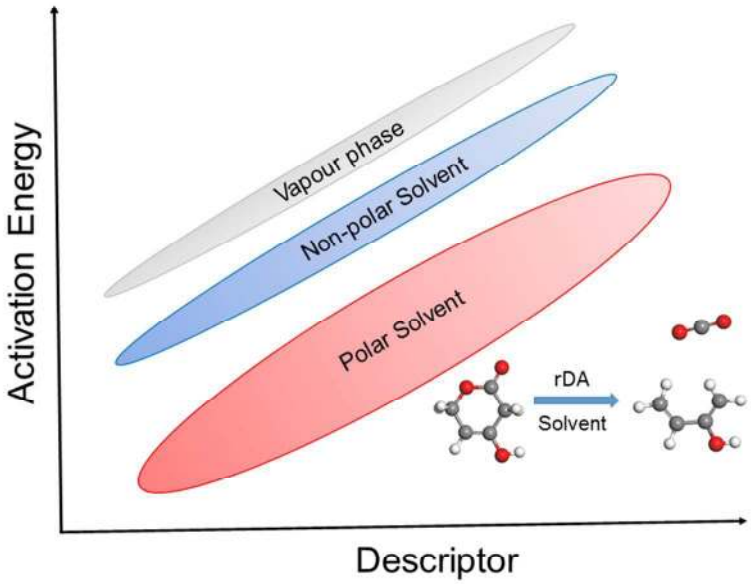

View Article Online
DOI: 10.1039/C6RA22303F

Abstract

Retro-Diels-Alder (rDA) reaction of partially saturated 2-pyrone molecules to form 1,3-butadiene backbone and CO_2 was studied using density functional theory (DFT) calculations in vapor-phase, polar and non-polar solvents. The activation barriers for the ring-opening and decarboxylation of the molecules was correlated to the type of substituent present on the 2-pyrone ring. In vapor-phase, the electronic effect of substituents led to a linear scaling relationship between the calculated activation barrier and corresponding frontier molecular orbital (FMO) gap of the product diene and CO_2. A new descriptor was proposed as the average of the ionization potential (IP) of the diene and the electron affinity (EA) of the dienophile to describe the activation energy trend. Solvents were calculated to reduce the activation barriers by stabilizing the polar transition state by as much as 40 kJ/mol, wherein polar solvents were calculated to reduce the barrier more than the non-polar solvents. The rDA reaction activation barrier in the solvent decreases in the following order vapor-phase > n-hexane > benzene > acetone > methanol > water. The effect of solvents in rDA reactivity trends was successfully described for the first time through a single descriptor, the FMO gap. Existence of Brønsted-Evans-Polanyi (BEP) relationship was established for the rDA reaction over different solvents. In solvents the FMO gap, $(IP_{diene}+EA_{dienophile})/2$ and BEP relationship were proposed as the reactivity descriptors for the rDA reaction of 2-pyrones.

Keywords*: FMO gap, retro-Diels-Alder reaction, reactivity descriptors, ionization potential, electron affinity, solvent effect, BEP relationship, 2-pyrones, ring-opening, decarboxylation*

Introduction

Biomass-derived lactones are known to be an important class of potential platform molecules which can be upgraded to produce fuels and chemicals[1–5]. 2-Pyrones are α, β unsaturated six

View Article Online
DOI: 10.1039/C6RA22303F

membered lactones, which are produced from the fermentation of biomass or biomass-derived aqueous sugars via polyketide synthesis routes[6,7], and are used as precursors to produce commodity chemicals, fuels and bioactive molecules like pheromones, coumarins, solanopyrones etc.[8–10]. In recent studies, triacetic acid lactone (TAL) is suggested to produce a number of useful products such as 1,3-pentadiene, parasorbic acid, hexenoic acid, 2,4-pentanedione and sorbic acid via a combination of ring-opening, decarboxylation, hydrogenation and dehydration reactions[10].

The ring-opening and decarboxylation in general is a key step involved in biological processes such as Krebs cycle, and in synthetic organic chemistry to produce intermediate and commodity chemicals via CO_2 elimination from biomass oxygenates.[11] Partially saturated 2-pyrones with a double bond at C_4-C_5 position were observed to undergo ring-opening and decarboxylation through rDA reaction under mild condition (T<423 K) yielding the substituted 1,3-butadiene backbone and CO_2[10]. Interestingly, compared to the ring-opening and decarboxylation of lactones, the rDA reaction was observed to proceed in water without the requirement of an acid catalyst. The biological synthesis procedures of 2-pyrones could be augmented with metabolic pathway engineering to get a desired substituent on the 2-pyrone ring which will lead to the formation of a target product.[12]. Thus, on synthesizing similar partially saturated 2-pyrones with different types of substituent and subsequent catalytic transformation via rDA reaction at mild condition will lead to the discovery of novel routes for the production of bio-renewable chemicals and fuels.

Descriptors are commonly used to understand the reactivity trends between molecules both in homogeneous and heterogeneous reaction.[10,12–17] Nandi *et al*. have utilized a quantitative structure-activation barrier relationship (QSABR) model to obtain a universal descriptor for DA

View Article Online
DOI: 10.1039/C6RA22303F

reaction.[13] The descriptor proposed by the authors consisted of several physical descriptors such as softness, hardness, electronegativity, electrophilicity of diene and dienophiles. On a closer look, it can be deduced that the different descriptors used in the universal relationship are indirectly related to the HOMO (highest occupied molecular orbital) and LUMO (lowest unoccupied molecular orbital) of the constituent diene and dienophile. In a simplifying approach, the author could possibly have used HOMO and LUMO energies as the descriptor. Both Chia *et al*.[10] and Gupta *et al*.[12] have used FMO gaps to explain trends observed in the vapor-phase rDA reaction to correlate with the experimentally measured and/or density functional theory (DFT) calculated activation barrier of partially saturated 2-pyrones; however the authors were unable to explain the activation barriers for the same molecules undergoing rDA reaction in polar and non-polar solvents. Gupta *et al*. have further proposed steric factor and positioning of the –Me substituent to the ring, to play a significant role in determining the activation barrier, which cannot be explained through FMO gap. Therefore, this study is focused on studying the effect of substituents at a specified (C_4) position of the molecule (Figure 1) on the resultant FMO gap and the computed activation barriers for ring-opening and decarboxylation via the rDA reaction, where –Me, -OH, -OMe, -NH_2, -CHO and –CO_2Me refers to methyl, hydroxyl, methoxy, amine, formyl, acetate functional group, respectively. The activation energies of rDA reaction in vapor phase are plotted versus the FMO gap to obtain linear scaling relationship which can describe the reactivity trends for the model partially-saturated 2-pyrones.

View Article Online
DOI: 10.1039/C6RA22303F

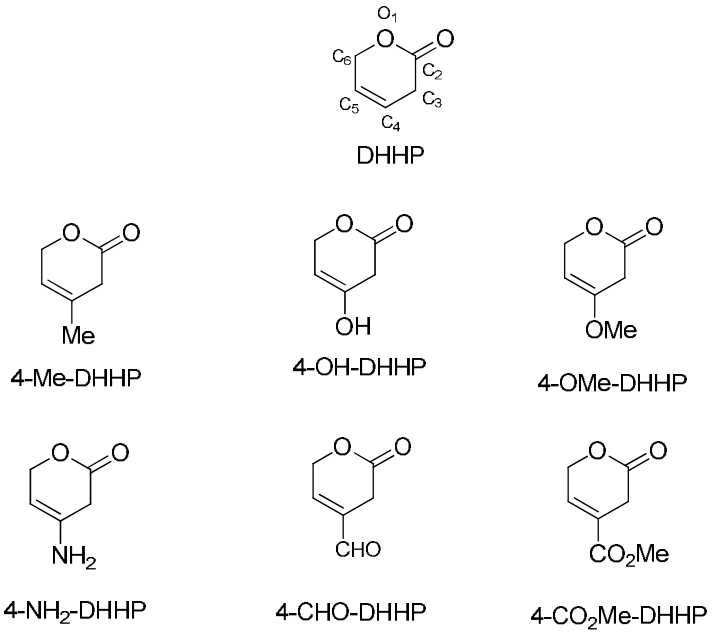

Figure 1. Molecular structures of partially saturated 2-pyrones with electron donating and electron withdrawing substituent at C_4.

Understanding the effect of solvent in DA and rDA reaction has been a continued interest in scientific community over the years. Desimoni *et al.*[18] investigated the solvent effect in DA reaction and suggested hyperbolic correlation of the reaction rate in different solvents with the acceptance number of the solvents[19], which was correlated to the LUMO of the solvent. Wang *et al.*[20] have utilized DFT calculations of DA reaction between *o*-quinone methides and various substituted ethenes to study the selectivity and reactivity trends. The authors observed that the activation barrier got reduced when the reaction was performed in solvent with high dielectric constant. However, a one-to-one linear scaling relationship was not obtained. Underlying fundamental factors affecting rDA reactivity in polar and non-polar solvents have not been investigated in detail. Wijnen *et al.*[21] studied rDA reaction in water and suggested two primary factors for the increase of rate in water; first was the stabilization of the TS due to H-bonding with the polarized TS relative to the reactant state, second was the lower hydrophobic interaction

View Article Online
DOI: 10.1039/C6RA22303F

of the TS compared to the reactant. The authors have obtained linear scaling relationship between the activation barriers of the rDA reaction in different solvents correlating to the solvent polarity.

In solvent for both DA and rDA reactions, the activation energy was observed to be difficult to correlate with a single suitable descriptor, likely due to the differential polarization of the activated complex and the reactant by the solvent[18,21–25]. To our knowledge, a single descriptor describing the reactivity trends over a range of non-polar and polar solvents correlating with the electronic or substituent effect in rDA reaction remains to be established. In this study, an attempt is made to search for a single reactivity descriptor for the rDA reaction of partially saturated 2-pyrones with both electron donating and electron withdrawing substituent and covering a range of five solvents with different dielectric constant, representing both polar and non-polar solvents. FMO gap is proposed as the unique descriptor which was able to explain the reactivity trends for rDA reaction with similar type of molecules over vapor-phase and solvents with reasonably good accuracy. To compare with, an alternate descriptor computed as the "average of the ionization potential (IP) of the diene and electron affinity (EA) of the dienophile, $\frac{IP_{diene}+EA_{CO_2}}{2}$," is presented, wherein a similar scaling relationship with activation energies is obtained. Both descriptors are likely to explain the electronic effects on reactivity trends for the rDA reactions of partially saturated 2-pyrones. In addition, Brønsted-Evans-Polanyi (BEP) relationship was explored between the activation energies and reaction energies of the 2-pyrones undergoing rDA reaction in vapor-phase and solvents. Thus, from the computational study, a molecular level design principle could be developed to understand novel processes, which are being experimented to convert new platform molecules into commodity products.

View Article Online
DOI: 10.1039/C6RA22303F

Computational method

DFT calculations based on DNP (double numerical plus polarization) numerical basis set were performed using the DMol^3 module as available in Material Studio 8 (Biovia, San Diego, USA)[26]. Generalized gradient approximation (GGA) with PW91 functional was used to describe the exchange correlation energy and potential[27]. PW91 functional has also been previously used for similar reaction to obtain good correlation with experimental trends.[2,10,12] rDA reaction of DHHP, 4-OH-DHHP and 4-CHO-DHHP were additionally simulated with dispersion-corrected GGA functionals[28]. Grimme DFT-D correction was applied in both PW91 and PBE[29] functional to check the change in the PESs of rDA reaction when dispersion was added to commonly used GGA functionals. The comparison between the result obtained for the activation and reaction energies calculations using the dispersion corrected GGA functionals are given in Table S2. In general both the activation and reaction energies for the rDA reaction were observed to vary negligibly on changing the functional. On applying the dispersion corrected GGA methods the activation energy was reduced within a range of 5-8 kJ/mol, which is within the error of GGA functionals. The activation barrier and reaction energy trend remains unchanged for the dispersion corrected DFT functionals. Convergence criterion for geometry optimization and transition state (TS) search calculations were set with respect to energy, force and atom displacement respectively as; 0.0001 eV, 0.05 eV/Å and 0.005 Å. The activation barriers for ring-opening and decarboxylation were calculated using TS search, performed by the linear synchronous transit/quadratic synchronous transit (LST/QST) method[30]. In LST a set of single point calculations were performed on a set of linearly interpolated structures between the reactant and the product. First estimate of TS structure was provided by the maximum energy structure along this path. The structure was subsequently refined in orthogonal direction to the

View Article Online
DOI: 10.1039/C6RA22303F

QST and used as an intermediate for QST pathway yielding a structure closer to the TS geometry. The structure thus obtained was further refined with the 'TS Optimization' module in DMol[3]. In TS optimization, the optimization started with the TS structure obtained from LST/QST method and searched for energy maxima along a normal mode using the Newton-Raphson line search algorithm. All the TS obtained in this study were verified by the presence of single imaginary frequency vibrational mode representing the reaction coordinate. Finding TS from this LST/QST method is extensively utilized in previous reports[2,12,31,32]. Energies of HOMO and LUMO of the reactants and products were obtained by checking the orbitals property tab in DMol[3].

The IP and EA of the dienes and dienophile was calculated by the definition given below[33];

$$\mathrm{IP} = \mathrm{E}_{\mathrm{cation}} - \mathrm{E}_{\mathrm{ground\ state}}$$

$$\mathrm{EA} = \mathrm{E}_{\mathrm{ground\ state}} - \mathrm{E}_{\mathrm{anion}}$$

Energies of the cations were obtained by assigning a +ve charge during the geometry optimization of the diene. Similarly energies of anions were obtained by assigning a –ve charge during geometry optimization. Solvent environment was simulated using conductor-like screening model (COSMO) in which solvents were represented by their respective dielectric constant; water (ε=78.54), methanol (ε= 32.63), acetone (ε= 20.70), benzene (ε= 2.28) and n-hexane (ε= 1.89).[34,35]

Rate constants and log(k) values were calculated for vapor-phase rDA reaction using the harmonic approximation of the transition state theory.[2,36,37] The values of activation energies and vibrational frequencies as calculated by DFT were used to calculate the rate constants, which is given by the following equation,

View Article Online
DOI: 10.1039/C6RA22303F

$$k_{HTST} = \frac{k_B T}{h} . \frac{\Pi_{i=1}^{D} (1 - e^{-\frac{h\nu_i^{\text{int}}}{k_B T}})}{\Pi_{j=1}^{D-1} (1 - e^{-\frac{h\nu_j^{*}}{k_B T}})} . e^{-\frac{(E^{*} - E^{\text{int}})}{k_B T}}$$

where, k_B is the Boltzmann constant, h is the Planck's constant, v_i^{int} and v_j^* corresponds to normal mode frequencies of the reactant and the transition state, respectively, E* is the energy of the transition state and E_{int} is the energy of the reactant state.

Results and discussion

The reaction diagram for vapor-phase ring-opening and decarboxylation of 3,6-dihydro-2H-pyran-2-one (DHHP) performed by us in our previous article is shown in Figure 2(a).[12] The rDA reaction follows a concerted route in which ring-opening and decarboxylation occur in one step yielding 1,3-butadiene and CO_2 with an activation energy of 135.7 kJ/mol. In contrast, some studies have suggested a two-step rDA reaction, involving the formation of a stable intermediate in polar solvents[12]. Structures of likely ionic intermediates formed on ring-opening of DHHP were optimized and found to be unstable in vapor-phase, which was the case for all the molecules studied. In a standard normal electron demand DA reaction between a diene and dienophile, the diene is electron rich and dienophile is electron deficient. The HOMO of the electron rich diene is higher in energy than the HOMO of the electron deficient dienophile; whereas LUMO of the dienophile is lower in energy than LUMO of the diene[38–40]. Hence during the DA reaction, the HOMO of the diene interacts with the LUMO of the dienophile and the reactivity is determined by the respective FMO gap ($HOMO_{diene}$-$LUMO_{dienophile}$). In the alternate case of inverse electron demand, diene could be electron deficient and dienophile could be electron rich and the LUMO of the diene and HOMO of the dienophile interact and the resultant FMO gap ($HOMO_{dienophile}$-$LUMO_{diene}$) can be correlated to the reactivity. Following the principle

View Article Online
DOI: 10.1039/C6RA22303F

of microscopic reversibility, the rDA reaction in this study is envisaged to follow the similar descriptor (FMO gap of the product diene and dienophile) to describe the reactivity. The FMO gap between the product diene and dienophile (CO_2) for normal electron demand (487.7 kJ/mol) was calculated to be lower than the inverse electron demand (692.1 kJ/mol) (Entry 1, Table 1). Similar trend in the normal electron demand gap were observed for all the molecules studied (Table 1), and thereby, normal electron demand gap was considered as the FMO gap.

View Article Online
DOI: 10.1039/C6RA22303F

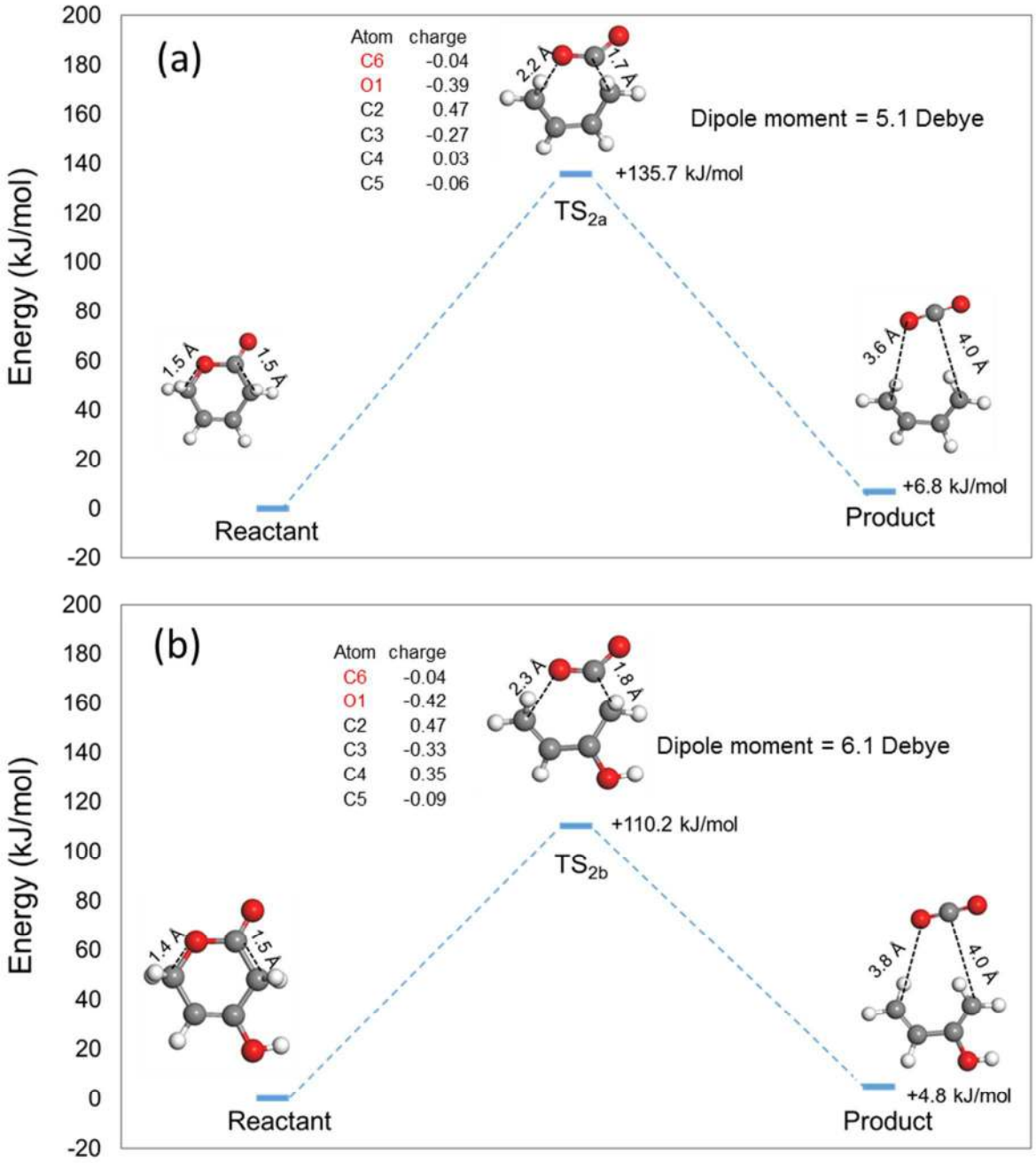

Figure 2. Reaction diagram for (a) rDA reaction of DHHP[12] and (b) 4-OH-DHHP showing the effect of electron donating substituent at C_4 on the activation energy, transition state, charge distribution and dipole moment

* All the energies presented here and elsewhere in the article are electronic energy of the corresponding systems.

View Article Online
DOI: 10.1039/C6RA22303F

Table 1. Normal and inverse electron demand FMO gap and corresponding activation energies for rDA reaction, in vapor-phase

Entry	Reactant	Product	Normal electron demand gap (kJ/mol)	Inverse electron demand gap (kJ/mol)	Activation energy (kJ/mol)
1	DHHP[12]	1,3-butadiene+CO_2	487.7	692.1	135.7
2	4-Me-DHHP	2-Me-1,3-butadiene+CO_2	482.8	731.1	129.6
3	4-OH-DHHP	2-OH-1,3-butadiene+CO_2	442.9	712.2	110.2
4	4-NH_2-DHHP[12]	2-NH_2-1,3-butadiene+CO_2	370.8	740.7	85.3
5	4-OMe-DHHP	2-OMe-1,3-butadiene+CO_2	450.9	729.0	113.6
6	4-CHO-DHHP	2-CHO-1,3-butadiene+CO_2	526.5	583.9	138.2
7	4-CO_2Me-DHHP	2-CO_2Me-1,3-butadiene+CO_2	527.0	633.5	145.6

On substituting a –OH group at C_4 position of the DHHP, the FMO gap was calculated to be reduced to a value of 442.9 kJ/mol, Table 1, entry 3. The reduction in FMO gap is likely due to the presence of electron donating hydroxyl group which resulted into a reduced activation barrier of 110.2 kJ/mol for rDA reaction of 4-OH-DHHP yielding 2-OH-butadiene and CO_2 as shown in Figure 2(b), which is consistent with our recent study[12]. The reaction energies for ring-opening and decarboxylation of DHHP and 4-OH-DHHP were calculated to be 6.8 kJ/mol and 4.8 kJ/mol, respectively. Mulliken charge analysis (Table S8) of the transition state structures of DHHP and 4-OH-DHHP (TS_{2a} and TS_{2b}, respectively) showed that the C_6-O_1 polarization is higher for TS_{2b} ($C^{-0.04}$-$O^{-0.39}$) compared to TS_{2a} ($C^{-0.04}$-$O^{-0.42}$), as shown in Figure 2. Higher dipole

View Article Online
DOI: 10.1039/C6RA22303F

moment calculated for TS_{2b} (6.1 Debye) compared to TS_{2a} (5.1 Debye) also indicates higher polarity for TS_{2b}, Figure 2.

The electronic effect of substituent is explained by the FMO gap of the product diene (substituted 1,3-butadiene) and dienophile (CO_2)[12,18,38,40–42]. Substituting the hydrogen at C_4 with an electron donating group like OH decreases the FMO gap, whereas electron withdrawing substituent like –CHO are expected to increase the FMO gap. Lowering of FMO gap results in smaller activation barrier and higher reaction rates. Conversely, increase in FMO gap causes higher activation barrier and lower reaction rates[41]. Similar results were reported for the rDA reaction of substituted anthracene cycloadducts; wherein electron donating groups such as -OH, -OMe, -NH_2 and -NMe_2 at C_9 and C_{10} position were observed to accelerate the rate significantly and conversely electron withdrawing groups such as -NO_2, -CHO decreased the reaction rates.[43,44] In order to understand the electronic effect of the substituent, the study was expanded to include two more electron withdrawing (-CHO and –CO_2Me) substituent and three more electron donating substituents (-Me, -OMe, -NH_2) at C_4 position (Figure 1). The C_4 position was strategically substituted to unravel the electronic effect from steric[12] and distortion[45] effect. The molecules undergo ring-opening and decarboxylation through concerted rDA reaction, yielding substituted 1,3-butadiene and CO_2 as the products. The FMO gaps related to product diene and dienophile (CO_2) of the three molecules with electron donating group, 4-Me-DHHP, 4-OMe-DHHP and 4-NH_2-DHHP were calculated to be 482.8 kJ/mol, 450.9 kJ/mol, and 370.8 kJ/mol respectively (Entry 2, 5 & 4, Table 1) and are observed to be smaller than DHHP (Entry 1, Table 1). For the compound with electron withdrawing group, 4-CHO-DHHP and 4-CO_2Me-DHHP, the FMO gap is 526.5 kJ/mol and 527.0 kJ/mol respectively, which are larger than DHHP, Table 1. Activation energies for the three molecules with electron donating group, 4-Me-DHHP, 4-

View Article Online
DOI: 10.1039/C6RA22303F

OMe-DHHP and 4-NH_2-DHHP obtained are 129.6 kJ/mol, 113.6 kJ/mol and 85.3 kJ/mol respectively, which are smaller than DHHP (Entry 2, 5 & 4, Table 1). Whereas, for electron withdrawing groups 4-CHO-DHHP and 4-CO_2Me-DHHP, the calculated activation energies are 138.2 kJ/mol and 145.6 kJ/mol respectively, which are greater than DHHP. Rate constants calculated from simple harmonic transition state theory assumption (Table S1) matches to the trends discussed above, $k_{(4\text{-NH2-DHHP})} > k_{(4\text{-OMe-DHHP})} \sim k_{(4\text{-OH-DHHP})} > k_{(4\text{-Me-DHHP})} > k_{DHHP} \sim k_{4\text{-CHO-DHHP}} > k_{(4\text{-CO2Me-DHHP}),}$ where k is the rate constants for the 2-pyrones rDA reaction.

Parr *et al*.[15] have derived the electrophilicity ω, from the second order energy expression, in terms of variation in number of electrons, given as the expression, $\omega = \frac{\mu^2}{2\eta}$, where $\mu \approx \frac{(E_{HOMO} + E_{LUMO})}{2}$ and $\eta \approx E_{LUMO} - E_{HOMO}$. This shows that the global electrophilicity index can also be expressed as a function of HOMO and LUMO energies of the molecules. Pérez *et al*. used global electrophilicity index to explain reactivity and selectivity trends in several organic reactions, e.g. DA cycloaddition, Lewis acid catalyzed DA reactions and in 1,3-dipolar cycloaddition reactions.[46] The authors obtained an empirical relationship between the electrophilicity and rate constants for hydrolysis of the carbenium ions and addition of the nucleophiles to the C=C double bond. The authors have discussed the substituent effect on electrophilicity index, deriving an empirical formula correlating the Hammett substituent parameter (σ_p) to the electrophilicity index. Morell *et al*.[47] have used the universal reactivity-selectivity descriptor derived from Fukui function, to explain the regio-selective addition of electrophiles to an asymmetric alkene, regio-selectivity of DA reactions, basicity of cyclopendadienes, regio-selectivity of electrophilic aromatic substitution, reactivity of ketones and aldehydes towards base and nucleophiles.

View Article Online
DOI: 10.1039/C6RA22303F

In order to search for a simple and universal descriptor for rDA reaction, FMO gap was explored as the descriptor to explain the reactivity trends of the rDA reaction. The activation energies for rDA reaction of partially saturated 2-pyrones and corresponding FMO gaps of the resultant product diene and dienophile were plotted to obtain the linear scaling relationship between the two as shown in Figure 3. An increase in the FMO gap resulted into an increase in the activation energies for the rDA reaction. Good fitting parameters, with R^2 value 0.96 (Table S5) is obtained between the FMO gap and activation energies. Thus, similar to the DA reaction, FMO gap can be used as an activity descriptor for rDA reactions.

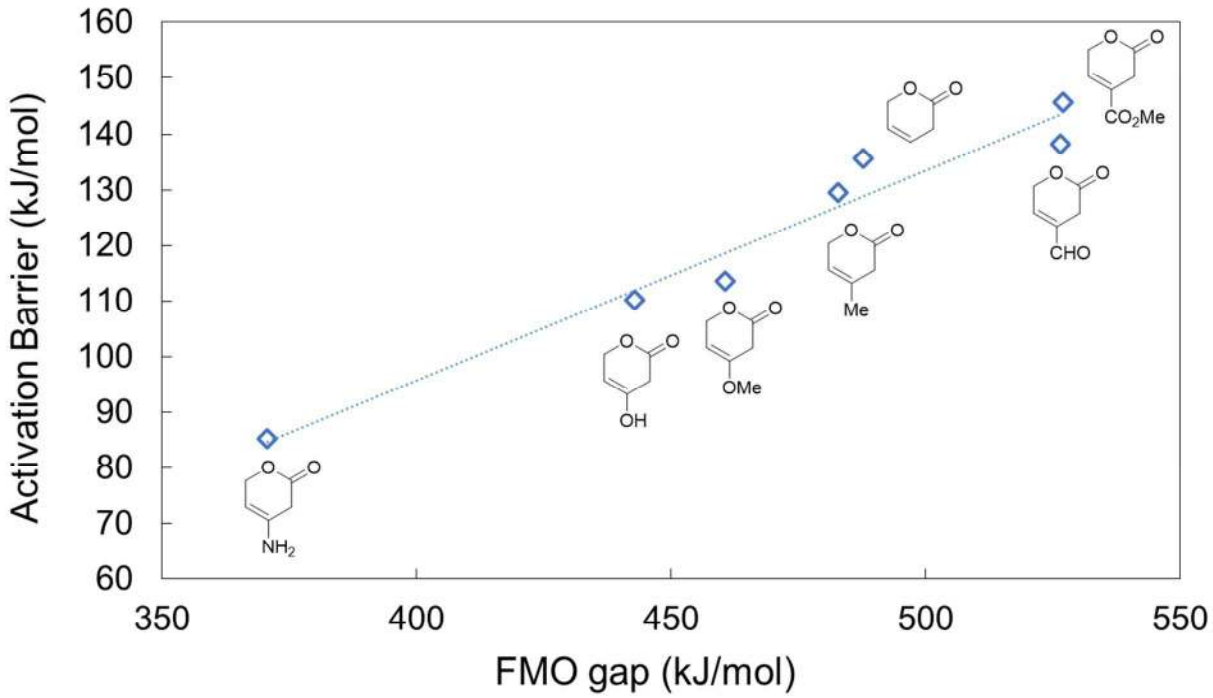

Figure 3. Scaling relation plot for FMO gap and activation barrier of the rDA reaction of partially saturated 2-pyrones

In search for an alternate reactivity descriptor for rDA reaction rates, another reactivity descriptor was explored. In normal DA reaction, the diene donates electron and dienophile accepts it, thus IP of the diene and EA of the dienophile can possibly be a descriptor for the reactivity of rDA

View Article Online
DOI: 10.1039/C6RA22303F

reactions. The IP of the product dienes and EA of CO_2 obtained from the rDA reaction are given in Table 2. A common trend was observed for the IP of the dienes. The IP of the molecules with electron donating group, were observed to be lower than the one with electron withdrawing group. For example, IP of 2-OH-1,3-butadiene was calculated to be 791.8 kJ/mol, which was lower than the IP of 1,3-butadiene (839.5 kJ/mol). Whereas, the IP of 2-CHO-1,3-butadiene is 859.8 kJ/mol, which was higher than 1,3-butadiene (Table 2). The activation energies for rDA reaction of partially saturated 2-pyrones with respect to the new descriptor, $\frac{IP_{diene}+EA_{CO_2}}{2}$, was plotted to obtain a linear scaling relationship (Figure 4). An increase in the descriptor values, $\frac{IP_{diene}+EA_{CO_2}}{2}$, results into an increase in the activation barriers for the rDA reactions of the molecules studied. While the new descriptor was observed to give a reasonable fit (R^2 = 0.90), the R^2 value was observed to be lesser than the fit obtained on using the FMO gap as the descriptor. Possible reason for poor fit for $\frac{IP_{diene}+EA_{CO_2}}{2}$ can be due to poor description of charged system by GGA in general.[48–50]

Table 2. Ionization potential (IP) and electron affinity (EA) values of the product dienes and dienophiles in vapor-phase

Entry	Molecules	Ionization Potential(IP) (kJ/mol)	Electron Affinity (EA) (kJ/mol)	$\frac{IP_{diene}+EA_{CO_2}}{2}$ (kJ/mol)
1	1,3-Butadiene	839.5	-79.6	374.6
2	2-Me-1,3-butadiene	809.9	-84.1	359.8
3	2-OH-1,3-butadiene	791.8	-77.5	350.7
4	2-NH_2-1,3-butadiene	711.0	-117.3	310.3
5	2-OMe-1,3-butadiene	772.5	-89.4	341.1
6	2-CHO-1,3-butadiene	859.8	43.6	384.7
7	2-CO_2Me-1,3-butadiene	834.8	22.7	372.1
8	CO_2	1319.9	-90.4	-

View Article Online
DOI: 10.1039/C6RA22303F

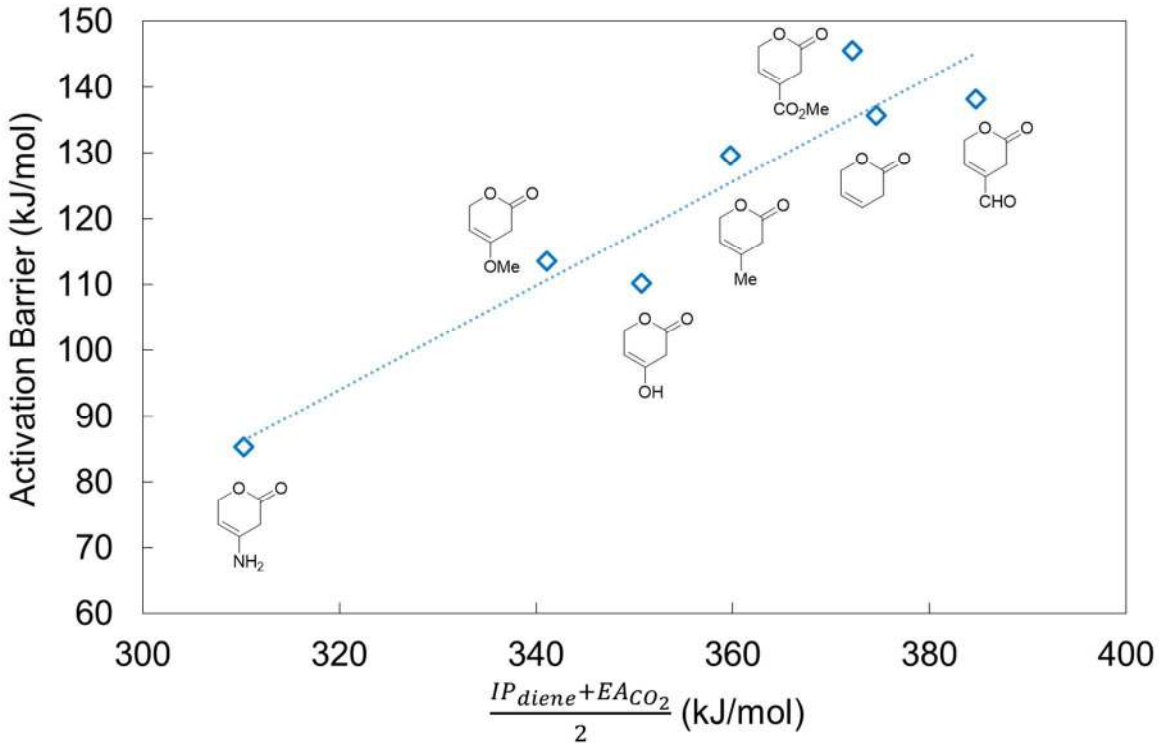

Figure 4. Scaling relation plot for the proposed descriptor, $\frac{IP_{diene}+EA_{CO_2}}{2}$, and activation barriers for the rDA reaction of partially saturated 2-pyrones

In order to gain a fundamental insight on the solvent effect in rDA reaction, the reaction was studied over five different solvents which include two non-polar and three polar solvents; n-hexane, benzene, acetone, methanol and water. Amongst the solvents n-hexane is non-polar with dielectric constant of 1.59; benzene is slightly more polar with a solvent dielectric constant value of 2.28; acetone, methanol and water are the three polar solvents with increasing dielectric constant 20.70, 32.63 and 78.54 respectively. Water and methanol are also known to form H-bonds. Sugimoto *et al*.[51] have performed rDA reaction of 4*H*-1,2-Benzoxazines to generate *o*-quinone methides in toluene, acetonitrile and dimethyl sulfoxide (DMSO), and observed a direct correlation between the activation barrier of the rDA reaction in a solvent to its dielectric

View Article Online
DOI: 10.1039/C6RA22303F

constant. The activation barrier was observed to decrease with the increase in the solvent polarity and the substituent effect was linearly correlated with σ_p.

Table 3. Reaction and activation energies for the rDA reaction of partially saturated 2-pyrones molecules in different solvents

Entry	2-pyrones[a]	Activation energies and reaction energies[c] (kJ/mol) in polar and non-polar solvents					
		vapor-phase	n-hexane (1.89)[b]	benzene (2.28)[b]	Acetone (20.70)[b]	Methanol (32.63)[b]	Water (78.54)[b]
1	DHHP	135.7 (6.8)	133.0 (12.7)	132.1 (14.3)	124.4 (25.0)	123.7 (25.6)	123.0 (26.4)
2	4-Me-DHHP	129.6 (10.1)	125.4 (16.3)	124.0 (18.0)	112.7 (29.2)	111.7 (29.9)	110.7 (30.7)
3	4-OH-DHHP	110.2 (4.8)	102.5 (10.4)	99.9 (12.0)	81.1 (22.1)	79.7 (22.8)	78.2 (23.5)
4	4-NH2-DHHP	85.3 (17.7)	73.8 (23.2)	70.4 (24.7)	47.1 (34.3)	45.7 (34.9)	44.2 (35.6)
5	4-OMe-DHHP	113.6 (5.6)	104.6 (11.1)	102.0 (12.7)	82.3 (22.8)	80.9 (23.4)	79.5 (24.1)
6	4-CHO-DHHP	138.2 (-4.9)	138.5 (1.7)	138.5 (3.5)	137.6 (14.6)	137.5 (15.3)	137.7 (16.0)
7	4-CO2Me-DHHP	145.6 (10.3)	145.0 (16.7)	144.8 (18.4)	142.0 (29.2)	141.2 (29.8)	140.8 (30.6)

[a] partially saturated; [b] dielectric constants of solvents; [c] numeric values within parenthesis show reaction energies in (kJ/mol)

Detailed reaction diagram for ring-opening and decarboxylation of 4-OH-DHHP in water is outlined in Figure 5. In polar solvent like water, 4-OH-DHHP may undergo the rDA reaction though a one-step concerted mechanism or a two-step mechanism via the formation of a zwitterionic intermediate. The activation and reaction energies for the partially saturated 2-pyrones were calculated for the rDA reaction for the concerted one step mechanism in all the solvents studied and are given in Table 3. The activation energies for the rDA reactions in the solvents phase are calculated to be lower than the vapor-phase. The TS being more polar in

View Article Online
DOI: 10.1039/C6RA22303F

nature, are more stabilized in solvents through the solvation energy and hence the activation energies are reduced.

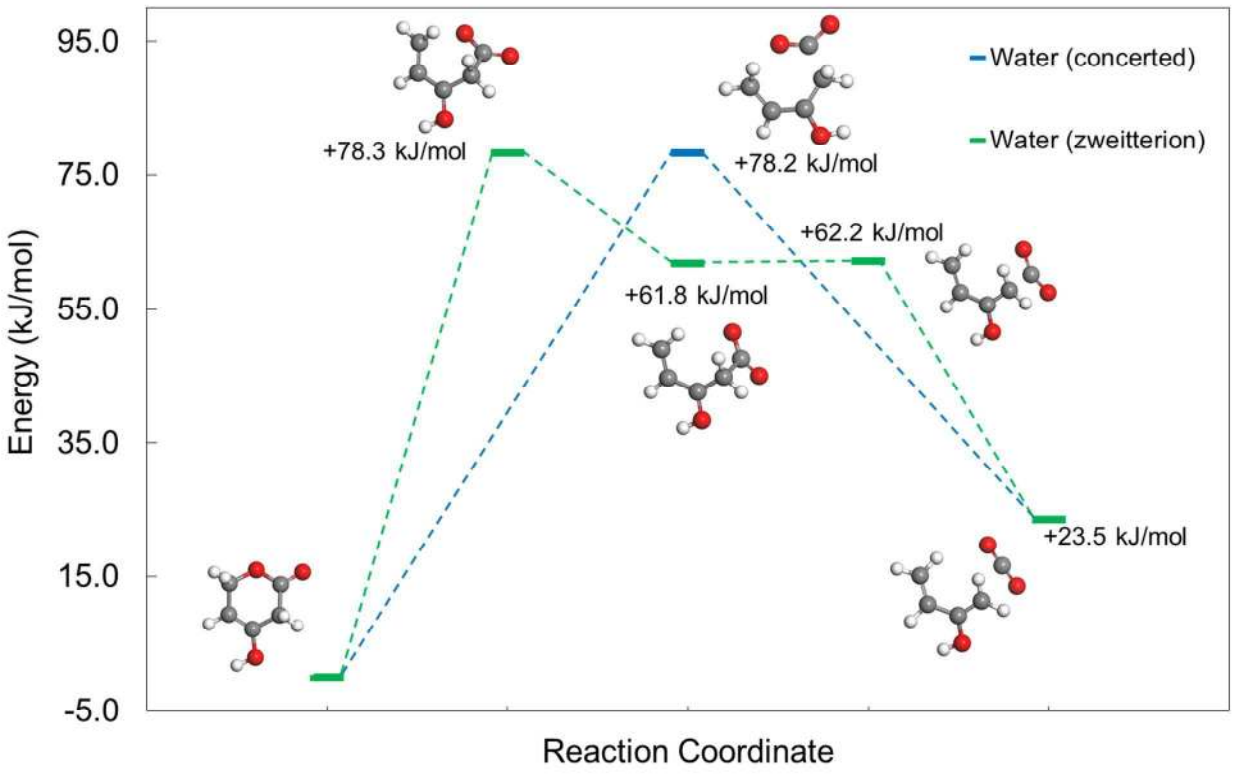

Figure 5. Reaction diagram for rDA reaction of 4-OH-DHHP in water (both concerted and through zwitterion intermediate)

Polar solvents can stabilize the polar TS more than the non-polar solvents and were able to reduce the activation energies further. The effect of solvent in reducing the activation barrier is more prominent for the 2-pyrones with electron donating group, whereas solvent has little or no effect for 2-pyrones with electron-withdrawing group. The reduction of activation energy from vapor-phase to water as medium is highest for 4-NH_2-DHHP (41.1 kJ/mol) followed by 4-OMe-DHHP (34.1 kJ/mol) and 4-OH-DHHP (32.0 kJ/mol). Whereas for electron withdrawing

View Article Online
DOI: 10.1039/C6RA22303F

substituent the activation energy was reduced marginally, 0.5 kJ/mol for 4-CHO-DHHP and only 4.8 kJ/mol for 4-CO_2Me-DHHP. The trend for the reduction of activation energy is explained through the polar nature of the TS, which is evident in Figure 6; wherein the activation energies calculated for the rDA reaction of the partially saturated 2-pyrones in different solvent medium was plotted against the dipole moment of their corresponding TS structures. The dipole moment of vapor-phase TS for 4-NH_2-DHHP (7.4 Debye), 4-OMe-DHHP (7.6 Debye) and 4-OH-DHHP (6.9 Debye) were calculated to be higher compared to DHHP (5.1 Debye), 4-CHO-DHHP (3.7 Debye) and 4-CO_2Me-DHHP (3.8 Debye) (Table S4). Similar trend was observed for all the five solvents studied. The dipole-moment of the TS for electron donating groups are likely to be higher due to the polar nature of the TS. As a general rule, it was observed that higher the dipole moment or polarity of the TS, higher is the stabilization through solvent medium and greater is the reduction in activation energy.

View Article Online
DOI: 10.1039/C6RA22303F

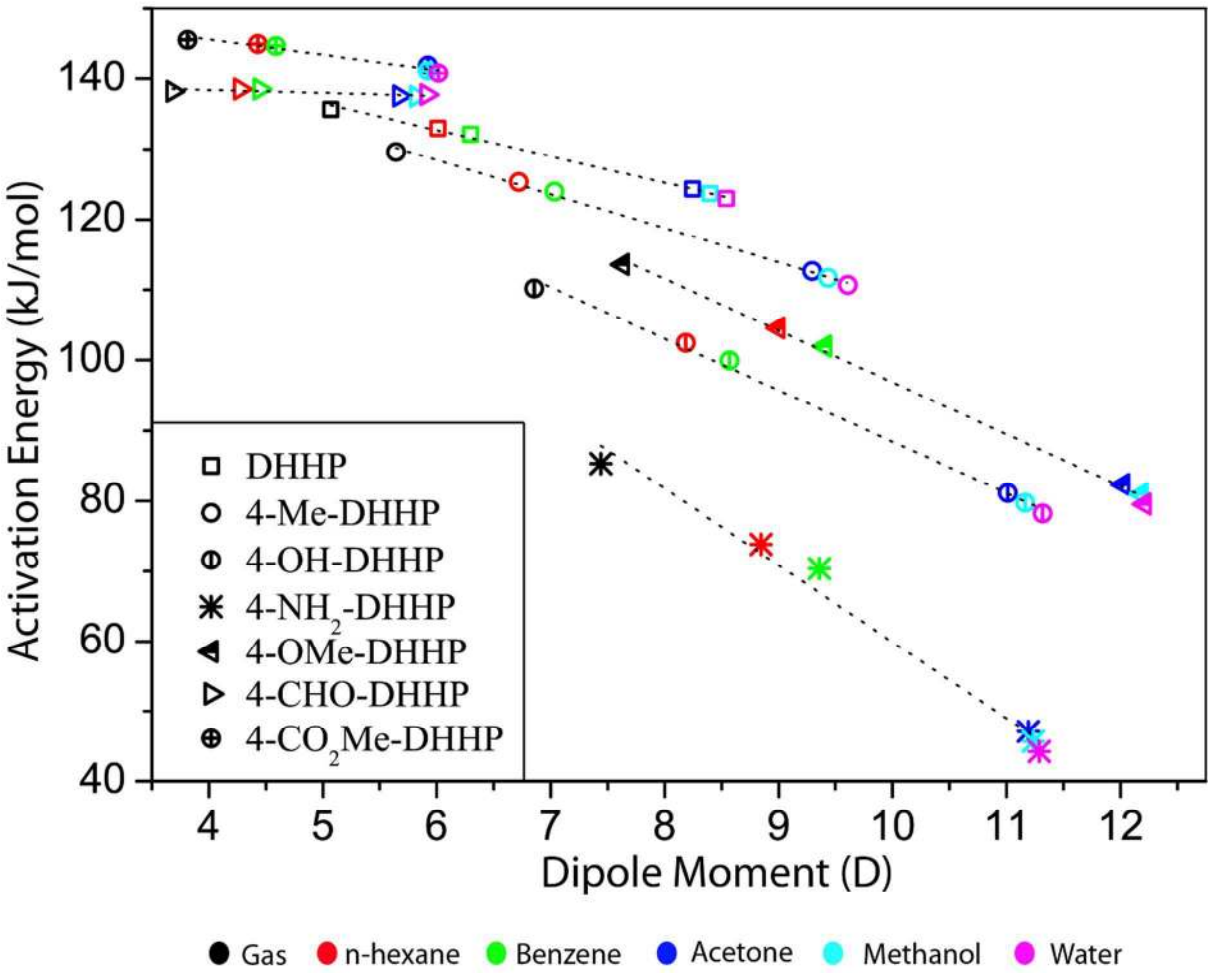

Figure 6. Scaling relationship plot between dipole moment at the transition state and activation barrier for the rDA of partially saturated 2-pyrones molecules in different solvents

In earlier studies, the two-step rDA mechanism via the formation of a stable zwitterionic intermediate was suggested to be a possible low activation energy path for 2-pyrone ring-opening and decarboxylation in polar solvent[10,12]. Water and methanol are likely to stabilize the zwitterion intermediate through solvation and H-bonding. In contrast, non-polar solvents were unable to stabilize the zwitterion intermediates. Interestingly it was observed that, the zwitterion intermediate was stable in polar solvents only for 2-pyrones with electron donating substituents (-OH, -OMe and $-NH_2$) as shown in Figure 5 for 4-OH-DHHP. For non or moderate electron

View Article Online
DOI: 10.1039/C6RA22303F

donating groups like –H and –Me and for electron withdrawing substituents (-CHO and –CO_2Me) the zwitterion intermediate was observed to be unstable and inclined to revert back to the corresponding product state. The activation energies for rDA reaction via the two-step zwitterion intermediate and concerted one-step mechanism were found to be similar for all the three partially saturated 2-pyrones having electron donating group (-OH, -OMe and –NH_2), as can be seen by comparing the activation energy values in Table 3 and Table 4. All of the three polar solvents studied had similar effect in stabilizing the TS and have similar activation energies for all the 2-pyrones.

Table 4. Activation energies (Ea) for the rDA reaction of the partially saturated 2-pyrone molecules through the zwitterion intermediate in different polar solvents

Entry	2-pyrones[a]	Activation energies (kJ/mol) in polar solvents		
		Acetone	Methanol	Water
1	4-OH-DHHP	81.2	79.8	78.3
2	4-NH2-DHHP	47.0	45.5	44.0
3	4-OMe-DHHP	82.5	81.1	79.5

[a] partially saturated

Similar to the vapor-phase rDA reaction, FMO gap was explored as a suitable reactivity descriptor to explain the solvent effect. As shown in Figure 7, the activation energies of 2-pyrone rDA reaction in different solvent medium was plotted against their corresponding FMO gap of the vapor-phase. The slope, constant and fitting parameter for the linear scaling relationship obtained between the activation energy and the FMO gap for different solvents are listed in Table S6.

View Article Online
DOI: 10.1039/C6RA22303F

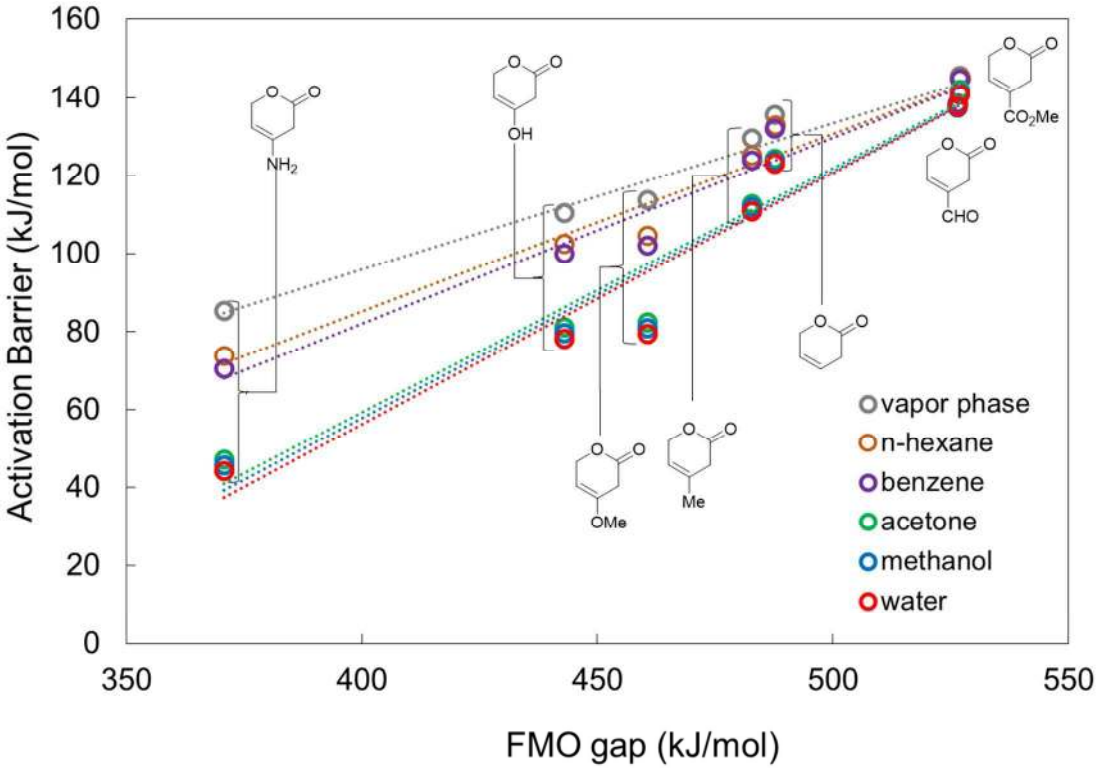

Figure 7. Scaling relation plot for FMO gap (at vapor-phase) and activation barrier for the rDA reaction of partially saturated 2-pyrones in different solvents.

In general, the slope of the scaling relation here increases with solvent polarity. The slope is lowest in vapor-phase and highest in water, and increases in the order, vapor-phase < n-hexane < benzene < acetone < methanol <water. Similarly, the constant becomes more negative on moving towards solvent with higher polarity, as seen in Table S6. As explained earlier, the TS being more polar than the initial state; the polar solvents result into a greater stabilization of the TS as compared to the non-polar solvents and hence increasing the slope of the linear scaling relations. It is evident from Figure 7, that FMO gap can be successfully used to explain the reactivity trends in different solvents as well. The larger reduction in activation energies for the molecules with electron donating substituents from vapor-phase and water compared to the ones with

View Article Online
DOI: 10.1039/C6RA22303F

electron withdrawing substituents discussed above was evident in different solvents as shown in Figure 7. Similar to FMO gap, $\frac{IP_{diene}+EA_{CO_2}}{2}$ can also be used as a descriptor to explain the activation energy trends for rDA reaction in solvent as well, shown in Figure 8. However the accuracy of fitting was found to be less for $\frac{IP_{diene}+EA_{CO_2}}{2}$ when compared to FMO gap as descriptor (Table S5).

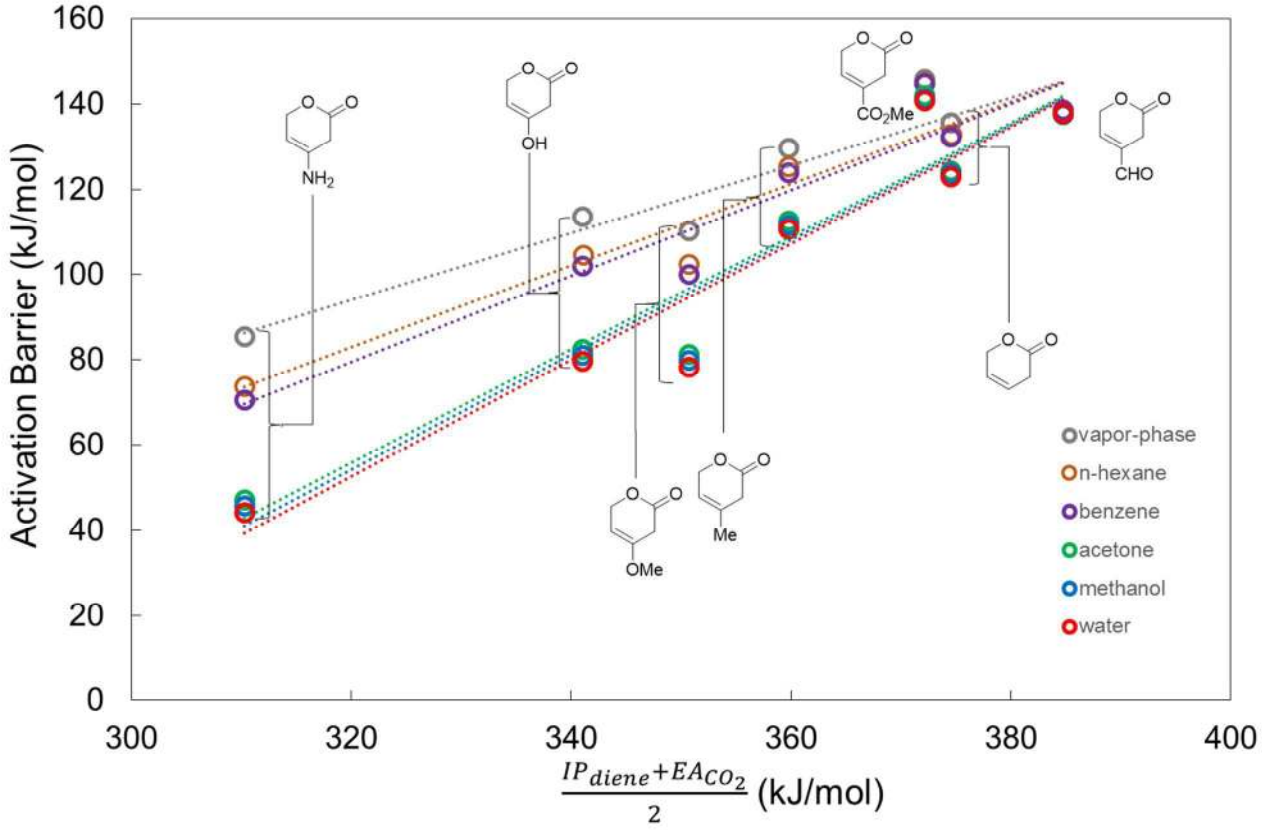

Figure 8. Scaling relation plot for $\frac{IP_{diene}+EA_{CO_2}}{2}$ (at vapor-phase) and activation barrier for the rDA reaction of partially saturated 2-pyrones in different solvents

View Article Online
DOI: 10.1039/C6RA22303F

Table 5 Change in the charge separation between C_6-O_1 of reactant and transition state in vapor-phase; and change in activation energies from vapor-phase to water as solvent medium

Entry	Molecules	$\delta Charge_{Reactant}$	$\delta Charge_{TS}$	$\delta Charge_{Reactant}$ - $\delta Charge_{TS}$	$Ea_{(vapor\text{-}phase)} - Ea_{(H2O)}$ (kJ/mol)
1	DHHP	0.56	0.35	0.21	12.7
2	4-Me-DHHP	0.55	0.36	0.19	18.9
3	4-OH-DHHP	0.55	0.38	0.17	32.0
4	4-NH_2-DHHP	0.53	0.39	0.14	41.1
5	4-OMe-DHHP	0.53	0.37	0.16	34.1
6	4-CHO-DHHP	0.56	0.34	0.22	0.5
7	4-CO_2Me-DHHP	0.56	0.35	0.21	4.8

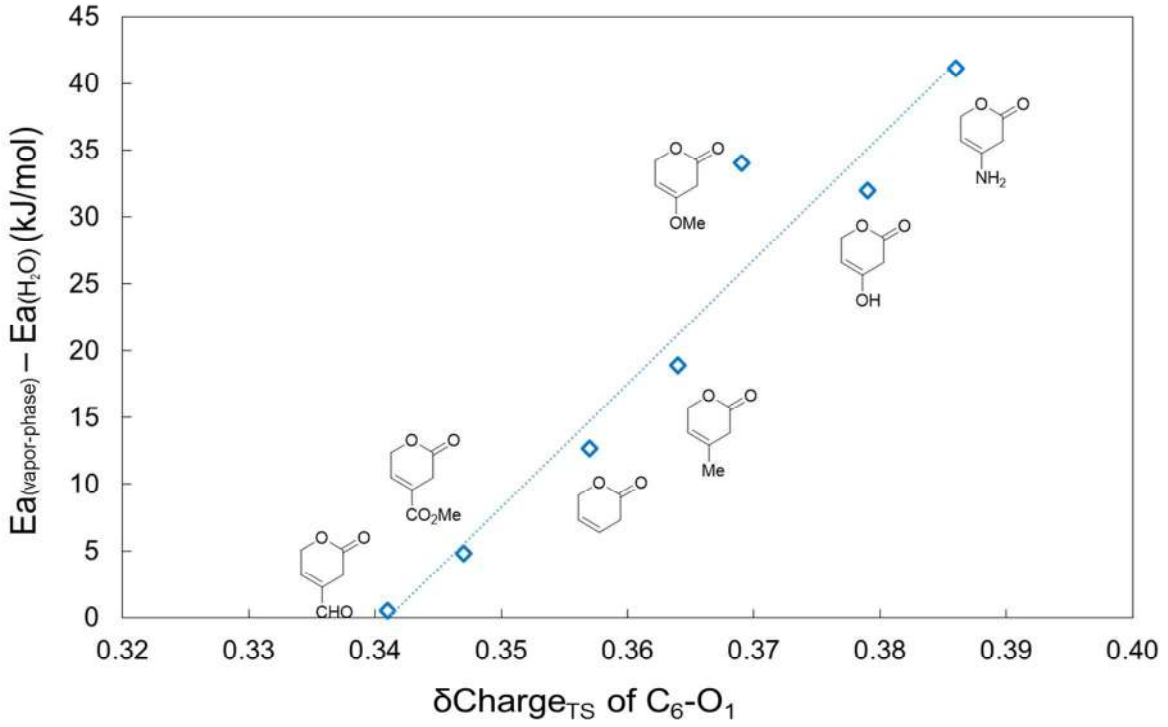

Figure 9. Scaling relationship plot between charge separation in TS "$\delta Charge_{TS}$ of C_6-O_1" and change in activation barrier (Table 5) from vapor-phase to water for the rDA reaction of partially saturated 2-pyrones.

View Article Online
DOI: 10.1039/C6RA22303F

The higher reduction in activation energy for the 2-pyrones with electron donating group due to the higher polar nature of their TS with electron donating group can be explained through the Mulliken analysis of charge separation between C_6-O_1 at the TS ($\delta Charge_{TS}$). Presence of electron donating group at the C_4 position increases the charge separation between C_6-O_1 at the TS (Table 5), 4-NH_2-DHHP (0.39), 4-OMe-DHHP (0.37) and 4-OH-DHHP (0.38) compared to DHHP (0.35), 4-CHO-DHHP (0.34) and 4-CO2Me-DHHP (0.35). Hence for 2-pyrones with electron donating substituent the TS structures are more stabilized compared to the DHHP and other 2-pyrones with electron withdrawing substituent. All of this results into an overall reduction of activation barriers for 2-pyrones with electron donating substituent compared to the electron withdrawing ones. A linear scaling relationship was obtained between the charge separation of C_6-O_1 at the TS in vapor-phase ($\delta Charge_{TS}$) and reduction in activation energy due to solvent effect ("$E_{a(vapor\text{-}phase)} - E_{a(H_2O)}$") is shown in Figure 9, with $R^2 = 0.94$ (Table S5). Hence one can couple the FMO gap and $\delta Charge_{TS}$ to obtain a universal relationship explaining the rDA reactivity trends of partially saturated 2-pyrones.

BEP relationships describing the linear correlation between activation and reaction energies of the similar reactions over transition metal catalysts is studied commonly in both homogeneous and heterogeneous catalysis. Liu *et al*. have observed BEP relationship for their study on Diels-Alder reaction for different ring size of cycloalkenes, cyclopropane, cyclobutene, cyclopentene and cyclohexene reacting with four different dienes cyclopentadiene, 1,3-dimethoxybutadiene, 3,6-bis(trifluoromethyl)tetrazine and 3,6-dimethyltetrazine.[52] Similarly, Zhong *et al*. have obtained BEP correlation for uncatalyzed 1,4-hydrogenation of polycyclic aromatic

View Article Online
DOI: 10.1039/C6RA22303F

hydrocarbons (PAH), over different sizes of PAH's.[53] In Figure 10, the activation energy of the seven model unsaturated 2-pyrones undergoing rDA reaction in vapor-phase, polar and non-polar solvents is plotted against their corresponding reaction energies to obtain the BEP scaling relationship. The BEP scaling with the corresponding slope and constants of the molecules studied are given in Table 6. Model structures with electron donating substituent (-Me, -OH, -OMe and $–NH_2$) showed a higher slope compared to the structures with electron withdrawing groups (-CHO and $–CO_2Me$). In general, higher the electron donating capacity of the substituent, higher was the slope in BEP linear scaling. For electron withdrawing group, negligible effect of the solvent was observed, which was evident in the BEP scaling plot. Thus, the effect of solvent in rDA reaction reactivity trends was successfully described by the BEP relationship.

Table 6. Slope and constants for BEP scaling relationship between the reaction energies and activation energies for the rDA reaction of partially saturated 2-pyrone in different solvents.

Entry	2-pyrones[b]	Slope (α)	Constant (β)
1	DHHP	-0.67	141
2	4-Me-DHHP	-0.94	140.1
3	4-OH-DHHP	-1.75	120
4	4-NH_2-DHHP	-2.34	127.6
5	4-OMe-DHHP	-1.87	124.9
6	4-CHO-DHHP	-0.04	138.3
7	4-CO2Me-DHHP	-0.24	148.7

[b] BEP scaling relationship

View Article Online
DOI: 10.1039/C6RA22303F

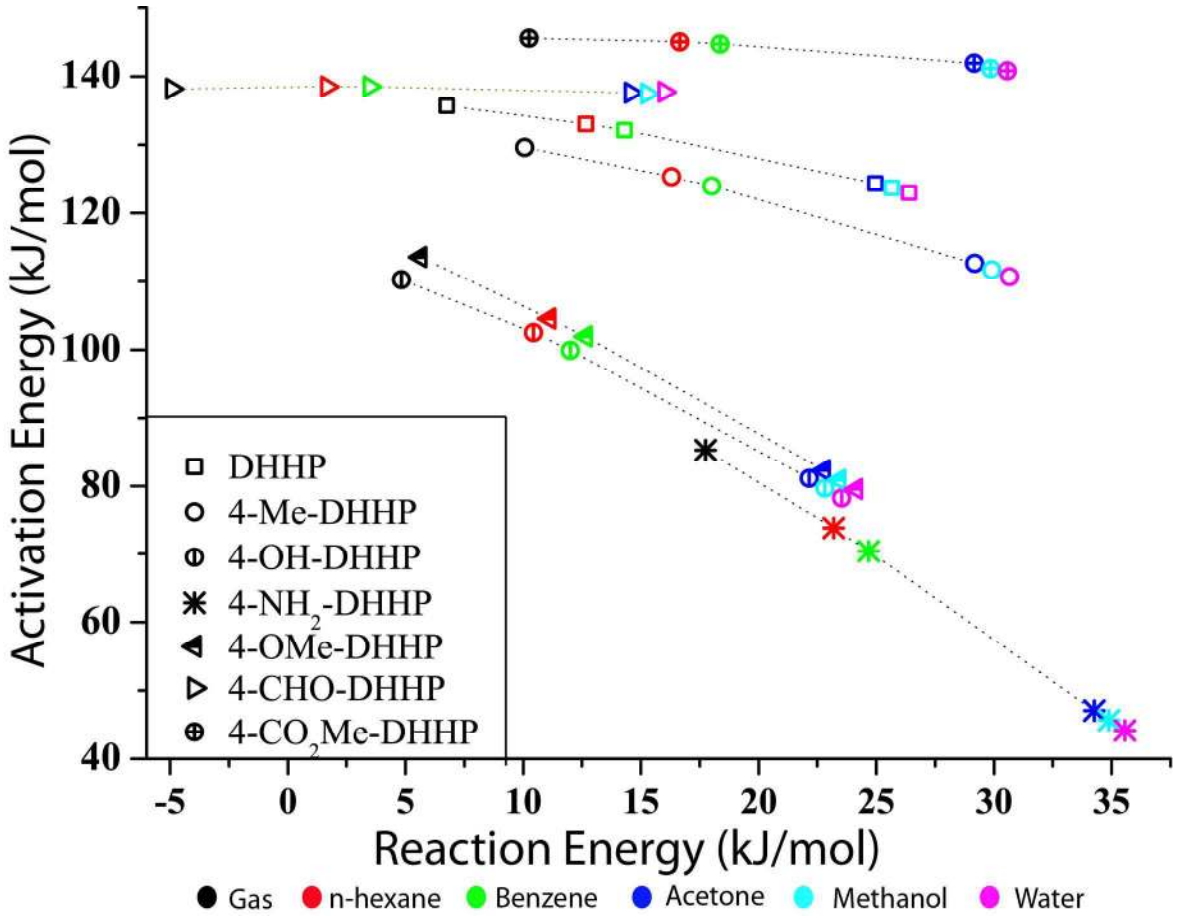

Figure 10. BEP scaling relationship between the reaction energy and activation barriers for rDA reaction of partially saturated 2-pyrones in different solvents.

Conclusion

Vapor-phase rDA reaction of partially saturated model 2-pyrones was studied using DFT to understand the electronic effect of substituent on FMO gap and corresponding activation barriers. The principle underlining the normal electron demand and inverse electron demand FMO gap for a DA or rDA reaction was explained through DFT. Presence of an electron donating group at C_4 position of the molecule was observed to decrease the FMO gap, resulting into a decrease in the activation barrier of the rDA reaction. This causes an increase in the reaction rates for these molecules. Conversely, presence of electron withdrawing group at C_4 position was observed to

View Article Online
DOI: 10.1039/C6RA22303F

increase the FMO gap and thus the activation barrier of the reaction, consequently decreasing the overall rDA reaction rates. A linear scaling relationship between the activation barrier and FMO gap was obtained, explaining the underlying relationship between the two. A similar linear scaling relationship was obtained by plotting the activation energies versus the new proposed descriptor, $\frac{IP_{diene}+EA_{CO_2}}{2}$. The electronic effect of substituents in vapor-phase rDA reaction of partially saturated 2-pyrones were explained by both the descriptors. In order to understand the effect of solvent in rDA reaction, DFT calculations were performed to study rDA reaction in two non-polar and three polar solvents having different dielectric constants. Solvents in general were observed to reduce the activation barriers for the rDA reaction, with polar solvent reducing the barriers more than non-polar solvents. TS structures of the rDA reaction being more polar in nature compared to their corresponding reactant state were calculated to be differentially stabilized in solvents, thereby lowering the activation barriers. The effect of solvent was prominent for 2-pyrones with electron donating substituent compared to the electron withdrawing one. Highest reduction in activation barrier was obtained for 4-NH_2-DHHP (~ 40 kJ/mol) and lowest for 4-CHO-DHHP (~ 0 kJ/mol) when changing the rDA reaction medium from vapor-phase to water as solvent. The amount of reduction in activation barriers was correlated to the electron donating ability of the substituent. In general, higher electron donating ability resulted into a higher reduction in activation barrier. BEP relationships obtained for the molecules studied were observed to successfully correlate the activation and reaction energies of rDA reaction in vapor-phase and the five solvents. Though BEP relation is common for transition metal catalysis, this correlation has not been explored much for non-catalytic thermal reactions. The study shows that the BEP relationship can also be applied for a catalyst free rDA reaction to describe the activation energies.

View Article Online
DOI: 10.1039/C6RA22303F

In search for a universal and simple reactivity descriptor for rDA reaction over different solvents, FMO gap and $\frac{IP_{diene}+EA_{CO_2}}{2}$ are proposed to describe the activation barrier trends over vapor-phase and all the five solvents tested here with good accuracy ($R^2 > 0.9$). To the best of our knowledge this is the first instance where the rDA reactivity trends over vapor-phase and different solvents have been successfully explained through a single descriptor. However, it need to be emphasized with caution here that both FMO gap and $\frac{IP_{diene}+EA_{CO_2}}{2}$, can only describe the substituent and solvent effect in rDA reactions, which are electronic in nature. The steric or constrain effects present in both DA and rDA reaction causing destabilization at the TS due to the steric repulsion of the substituents or the hybridization geometry of participating atoms cannot be fully explained by these descriptors. More detailed approaches presented by Levandowski *et al*.[45] using distortion energy as parameter or method of including steric effect proposed by Gupta *et al*.[12] should be undertaken. As a hypothesis, FMO gap and distortion energy can be coupled together to obtain a universal descriptor for rDA and DA reaction.

Finally, the computational study presented here on the reactivity trend of partially saturated 2-pyrones using the linear scaling relationship, underscore the effectiveness of simple computational DFT methods in understanding common chemical reactions. The study shows how commonly encountered trends in chemical reactions can be understood and explained through already known descriptors and how new descriptors can be assigned. In designing a novel reaction, the two proposed descriptors can be used for predicting reactivity of an unknown molecule of similar type, undergoing rDA reaction in a range of solvents.

View Article Online
DOI: 10.1039/C6RA22303F

Acknowledgement

The financial support from the Department of Biotechnology (BT/COE/34/SP15097/2015), Government of India is acknowledged to carry out this work. MIA thanks Science and Engineering Research Board (PDF/2015/001040), Government of India for the financial support. Authors acknowledge the computer service center of Indian Institute of Technology, Delhi for providing the high performance computing systems.

References:

1 J. Q. Bond, D. M. Alonso, R. M. West and J. A. Dumesic, *Langmuir*, 2010, **26**, 16291–8.

2 S. Gupta, R. Arora, N. Sinha, M. I. Alam and M. A. Haider, *RSC Adv.*, 2016, **6**, 12932–12942.

3 M. I. Alam, S. Gupta, E. Ahmad and M. A. Haider, in *Sustainable Catalytic Processes*, eds. B. Saha, M. Fan and J. Wang, Elsevier B.V., 2015, pp. 157–177.

4 E. Ahmad, M. I. Alam, K. K. Pant and M. A. Haider, *Green Chem.*, 2016, **18**, 4804.

5 S. K. Bardhan, S. Gupta, M. E. Gorman and M. A. Haider, *Renew. Sustain. Energy Rev.*, 2015, **51**, 506–520.

6 D. Xie, Z. Shao, J. Achkar, W. Zha, J. W. Frost and H. Zhao, *Biotechnol. Bioeng.*, 2006, **93**, 727–736.

7 M. Nakajima, Y. Nishino, M. Tamura, K. Mase, E. Masai, Y. Otsuka, M. Nakamura, K. Sato, M. Fukuda, K. Shigehara, S. Ohara, Y. Katayama and S. Kajita, *Metab. Eng.*, 2009, **11**, 213–220.

8 G. P. Mcglacken and I. J. S. Fairlamb, *Nat. Prod. Rep.*, 2005, **22**, 369–385.

View Article Online
DOI: 10.1039/C6RA22303F

9 J. S. Lee, *Mar. Drugs*, 2015, **13**, 1581–1620.

10 M. Chia, M. A. Haider, G. Pollock, G. A. Kraus, M. Neurock and J. A. Dumesic, *J. Am. Chem. Soc.*, 2013, **135**, 5699–708.

11 D. L. Nelson and M. M. Cox, *Lehninger Principles of Biochemistry*, W H Freeman & Co, New York, 6th Editio., 2012.

12 S. Gupta, M. I. Alam, T. S. Khan, N. Sinha and M. A. Haider, *RSC Adv.*, 2016, **6**, 60433–60445.

13 S. Nandi, A. Monesi, V. Drgan, F. Merzel and M. Novič, *Chem. Cent. J.*, 2013, **7**, 171.

14 AlejandroToro-Labbé, Ed., *Theoretical aspects of chemical reactivity*, Elsevier, Amsterdam, The Netherlands, First edit., 2007.

15 R. G. Parr, L. V. Szentpály and S. Liu, *J. Am. Chem. Soc.*, 1999, **121**, 1922–1924.

16 H. Mayr and M. Patz, *Angew. Chemie Int. Ed.*, 1994, **33**, 938–957.

17 M. Roth and H. Mayr, 1995, **165591**, 37–39.

18 G. Desimoni, G. Faita, P. Righetti, N. Tornaletti and M. Visigalli, *J. Chem. Soc. Perkin Trans. II*, 1989, 437–441.

19 U. Mayer, V. Gutmann and W. Gerger, *Monatshefte fur Chemie*, 1975, **106**, 1235–1257.

20 H. Wang, Y. Wang, K. L. Han and X. J. Peng, *J. Org. Chem.*, 2005, **70**, 4910–4917.

21 J. W. Wijnen and J. B. F. N. Engberts, *J. Org. Chem.*, 1997, **62**, 2039–2044.

22 J. Chandrasekhar, S. Shariffskul and W. L. Jorgensen, *J. Phys. Chem. B*, 2002, **106**, 8078–8085.

23 J. F. Blake and W. L. Jorgensen, *J. Am. Chem. Soc.*, 1991, **113**, 7430–7432.

View Article Online
DOI: 10.1039/C6RA22303F

24 R. A. A. Foster and M. C. Willis, *Chem. Soc. Rev.*, 2013, **42**, 63–76.

25 L. R. Domingo and J. Andrés, *J. Org. Chem.*, 2003, **68**, 8662–8668.

26 B. Delley, *J. Chem. Phys.*, 1990, **92**, 508.

27 J. P. Perdew and Y. Wang, *Phys. Rev. B*, 1992, **45**, 244–248.

28 A. Karton and L. Goerigk, *J. Comput. Chem.*, 2015, **36**, 622–632.

29 J. P. Perdew, K. Burke and M. Ernzerhof, *Phys. Rev. Lett.*, 1996, **77**, 3865–3868.

30 T. A. Halgren and W. N. Lipscomb, *Chem. Phys. Lett.*, 1977, **49**, 225–232.

31 K. Shin, D. H. Kim, S. C. Yeo and H. M. Lee, *Catal. Today*, 2012, **185**, 94–98.

32 R. Liu, W. Shen, J. Zhang and M. Li, *Appl. Surf. Sci.*, 2008, **254**, 5706–5710.

33 J. C. Delgado, Y. Ishikawa and R. G. Selsby, *Photochem. Photobiol.*, 2009, **85**, 1286–1298.

34 A. Klamt and G. Schuurmann, *J. Chem. Soc. Perkin Trans. II.*, 1993, 799–805.

35 B. Delley, *Mol. Simul.*, 2006, **32**, 117–123.

36 T. J. Delph, P. Cao, H. S. Park and J. A. Zimmerman, *Model. Simul. Mater. Sci. Eng.*, 2013, **21**, 25010.

37 G. H. Vineyard, *J. Phys. Chem. Solids*, 1957, **3**, 121–127.

38 M. D. Rozeboom, I.-M. Tegmo-Larsson and K. N. Houk, *J. Org. Chem.*, 1981, **46**, 2338.

39 M. A. Mccarrick, Y. D. Wu and K. N. Houk, *J. Org. Chem.*, 1993, 3330–3343.

40 G. O. Jones and K. N. Houk, *J. Org. Chem.*, 2008, **73**, 1333–1342.

41 R. Sustmann, *Pure Appl. Chem.*, 1974, **40**, 569–593.

View Article Online
DOI: 10.1039/C6RA22303F

42 U. Pindur, G. Lutz and C. Otto, *Chem. Rev.*, 1993, **93**, 741–761.

43 Y. Chung, B. F. Duerr, T. a. McKelvey, P. Nanjappan and A. W. Czarnik, *J. Org. Chem.*, 1989, **54**, 1018–1032.

44 Y. S. Chung, B. F. Duerr, P. Nanjappan and A. W. Czarnik, *J. Org. Chem.*, 1988, **53**, 1334–1336.

45 B. J. Levandowski and K. N. Houk, *J. Org. Chem.*, 2015, **80**, 3530–3537.

46 P. Pérez, L. R. Domingo, A. Aizman and R. Contreras, in *Theoretical Aspects of Chemical Reactivity*, ed. AlejandroToro-Labbé, Elsevier, Amsterdam, Netherlands, First., 2007, pp. 139–202.

47 C. Morell, A. Grand, S. Gutiérrez-Oliva and Alejandro Toro-Labbé, in *Theoretical aspects of chemical reactivity*, ed. AlejandroToro-Labbé, Elsevier, Amsterdam, Netherlands, 2007, pp. 101–118.

48 A. J. Cohen, P. Mori-Sanchez, W. Yang, P. Mori-s, W. Yang, P. Mori-Sánchez and W. Yang, *Chem. Rev.*, 2012, **112**, 289–320.

49 M. C. Kim, H. Park, S. Son, E. Sim and K. Burke, *J. Phys. Chem. Lett.*, 2015, **6**, 3802–3807.

50 I. Bâldea, *Faraday Discuss.*, 2014, **174**, 37–56.

51 H. Sugimoto, S. Nakamura and T. Ohwada, *J. Org. Chem.*, 2007, **72**, 10088–10095.

52 F. Liu, R. S. Paton, S. Kim, Y. Liang and K. N. Houk, *J. Am. Chem. Soc.*, 2013, **135**, 15642–15649.

53 G. Zhong, B. Chan and L. Radom, *J. Mol. Struct. THEOCHEM*, 2007, **811**, 13–17.